Communication

# Self-Etching Reconstruction of Hierarchically Mesoporous F-TiO Hollow Microspherical Photocatalyst for Concurrent Membrane Water Purifications

Jia Hong Pan, Xiwang Zhang, Alan Jianhong Du, Darren D. Sun, and James O. Leckie

*J. Am. Chem. Soc.*, **2008**, 130 (34), 11256-11257 • DOI: 10.1021/ja803582m • Publication Date (Web): 05 August 2008



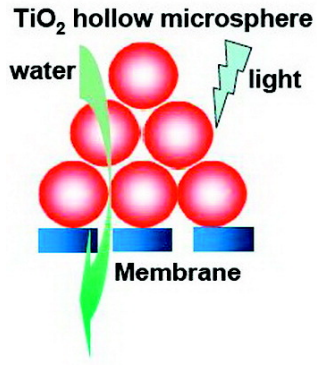


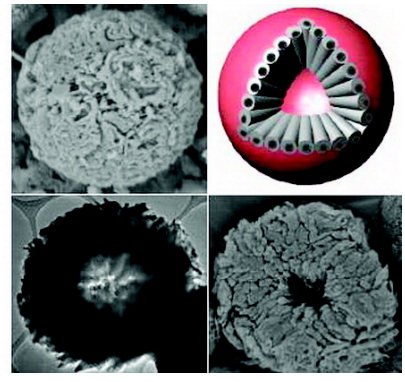

## More About This Article

Additional resources and features associated with this article are available within the HTML version:

- Supporting Information
- Links to the 1 articles that cite this article, as of the time of this article download
- Access to high resolution figures
- Links to articles and content related to this article
- Copyright permission to reproduce figures and/or text from this article

View the Full Text HTML

J|A|C|S
COMMUNICATIONS

Published on Web 08/05/2008

# Self-Etching Reconstruction of Hierarchically Mesoporous F-$TiO_2$ Hollow Microspherical Photocatalyst for Concurrent Membrane Water Purifications

Jia Hong Pan,*,† Xiwang Zhang,† Alan Jianhong Du,† Darren D. Sun,*,† and James O. Leckie‡

*School of Civil and Environmental Engineering, Nanyang Technological University, Singapore 639798, and Department of Civil and Environmental Engineering, Stanford University, Stanford, California 94305-4020*

Received May 14, 2008; E-mail: jhpan@ntu.edu.sg; ddsun@ntu.edu.sg

Hollow spherical metal oxides consisting of tailored nanobuilding units have recently attracted increasing attention in the fields of catalysis, adsorption, microreactors, and drug delivery.[1] This structural diversity at nano- and microscale leads to an array of unique physicochemical properties. A considerable fraction of this research has been devoted to $TiO_2$.[2−5] Recent progress shows that hollow $TiO_2$ spheres present enhanced performance in photocatalysis and photovaltaics due to their light scattering, organic adsorption, and porous characteristics.[3] Hollow $TiO_2$ nanospheres in the 0.1−0.6 $\mu$m diameter range have been produced by template-free one-pot synthesis under hydrothermal conditions. An Ostwald ripening mechanism has been proposed for these hollow nanospheres, and their photocatalytic property has been confirmed through removal of organic pollutants.[4,5]

Current trends for advanced water treatment combine concurrent low-pressure membrane filtration with photocatalysis; however, membrane fouling due to $TiO_2$ nanoparticles is the main obstacle.[6,7] Porous hollow $TiO_2$ microspheres reduce membrane fouling and result in a higher water production rate, and better water quality is an ideal candidate to practically achieve the technological integration of photocatalysis with membrane filtration for the advanced water purifications. Thus, the template-free pathway needs to be further developed for the large-scale production of hollow $TiO_2$ microspheres.

Here for the first time, we report a large-scale self-etching synthesis of monodisperse F-containing anatase $TiO_2$ hollow microspheres by hydrothermal treatment of $TiF_4$ in $H_2SO_4$ aqueous solution at 160 °C for 4 h. In our synthetic strategy, $H_2SO_4$ acts as an acid source to promote the HF etching. It also increases the ionic strength of the aqueous solution which governs the aggregation of hydrolyzed $TiO_2$ primary particles and the formation of porous microspheres. SEM and TEM measurements (Figure 1 and Supporting Information Figures S1−3) reveal the morphological evolution of our microspherical products with diameters of 1.8−2.5 $\mu$m synthesized in various $H_2SO_4$ solutions with mass concentrations from 0.1% to 1.0%. In 0.1% $H_2SO_4$ solution, slightly etched solid microspheres were shaped by aggregating several nanoflakes in the thickness of 20−40 nm (Figure 1a). An eroded hole appeared on each flake with the further increase of $H_2SO_4$ concentration (0.3%), as shown in Figure 1b. This corrosion on the surface of F−$TiO_2$ flakes is launched by the self-generated HF.[5] The surface of microspheres became smooth and their protuberances of the random packed nanoflakes disappeared due to the HF etching. The nanoflakes disintegrated and graduated away from the surface of the microspheres following the generation of erosive cavities at the elevated concentration of $H_2SO_4$, for example, 0.5 and 0.8% (Figure 1c,d). Finally, monodispersed mesoporous hollow F−$TiO_2$ microspheres with abundant cavities and nanopipes emerged in 1.0% $H_2SO_4$ solution (Figure 1e). BJH pore size distribution shown in Figure S4 further reveals that various mesopores in sizes of 2.0−10 nm exist, and the BET surface area is 21.6 $m^2/g$. A representative TEM micrograph (Figure 1f) indicates the resulting microspheres possess a hollow structure with a wall thickness of ca. 0.6 $\mu$m. This high ratio of hollow interior in the form of microsphere greatly decreases the density of F−$TiO_2$ microspheres, resulting in their high suspension in the water. The surfaces of hollow microspheres become rougher upon the enhanced HF etching, as compared with that of solid one (insert of Figure 1a). High-resolution TEM image (Figure S3) implies the synthesized hollow microspheres are fully crystallized in the anatase phase.

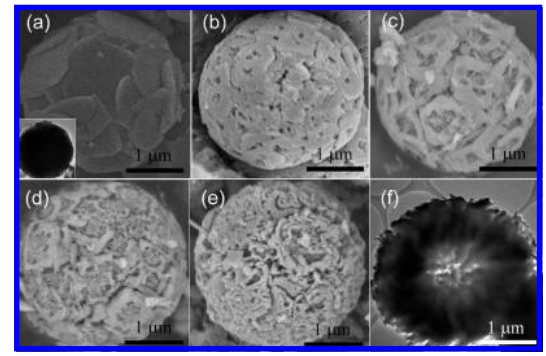


***Figure 1.*** SEM images of F-$TiO_2$ microspheres synthesized in (a) 0.1, (b) 0.3, (c) 0.5, (d) 0.8, and (e) 1.0% $H_2SO_4$ solution. Panel f and the insert of panel a are TEM images corresponding to hollow (e) and solid (a) microspheres, respectively.

XPS survey spectra (Figure S5a) indicate that all the microspheres synthesized in 0.1−1.0% $H_2SO_4$ contain Ti, O, F. The F/Ti atomic concentration ratio was 0.11 for solid microspheres and 0.16 for hollow ones. The concentration of F remarkably enhanced in hollow microspheres relates to the more serious HF etching. Similar trend was also found in the XRD analysis which indicated the hollow microspheres possess smaller anatase crystallites (Figure S6). Thus, evolutions in morphology, chemical composition, and crystal size of solid and hollow microspheres are derived from the enhanced HF etching with the increase of $H_2SO_4$ content. Figure S5b shows the high-resolution XPS spectra of F 1s. The only peak at 684.3 eV was assigned to the $F^-$ anions that are physically adsorbed on the surface of $TiO_2$ microspheres (≡Ti−F). The fluorination over the surface of $TiO_2$ may accelerate the photocatalytic degradation of a wide range of organic pollutants since the OH radicals generated on F−$TiO_2$ surface are more mobile than those generated on pure $TiO_2$.[8] On the other hand, the absence of F in the crystal lattice (BE = 688−689 eV) implies the oxygen in $TiO_2$ lattice is not substituted by F.

† Nanyang Technological University.
‡ Stanford University.


10.1021/ja803582m CCC: $40.75 

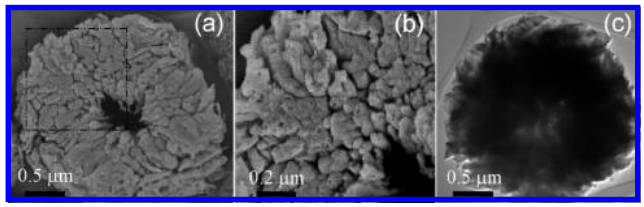


***Figure 2.*** SEM (a,b) and TEM (c) images of F−$TiO_2$ hollow hemispheres synthesized in 1.0% $H_2SO_4$ at 180 °C for 12 h.

To further understand the morphology and formation mechanism of our hollow microspheres, incomplete $TiO_2$ hollow microspheres with a circular opening were synthesized at the prolonged reaction time and higher reaction temperature (Figure S7). That is, $TiF_4$ in 1.0% $H_2SO_4$ solution was hydrothermally treated for 12 h at 180 °C to allow the operation of Ostwald ripening. Figure 2 panels a and b show the SEM images of representative microhemispheres. The wall of the synthesized hemispheres is around 400−700 nm, which is in good agreement with the TEM observation (Figure 2c). The building units of aggregated nanorods, which comprised additional hollow structures, are 300−600 nm in length and 40−60 nm in width. Several gaps (dark in Figure 2a,b) between the nanorods create accessible channels from hollow interior to exterior.

Clearly, hydrothermal reaction involves a dissolution−redeposition procedure. With the hydrolysis of $TiF_4$ in acid media, HF and $TiO_2$ gradually in situ release with a molar ratio of 4:1. The aggregated $TiO_2$ solid microspheres are chemically etched by corrosive HF, followed by the recrystallization of their surfaces. The accessible mesopore channels and corrosive nanorods are hence simultaneously generated. Moreover, the intruded HF may enrich at the center of the spheres, creating a hollow interior. Compared with the Ostwald ripening process for the hollow $TiO_2$ nanospheres synthesized in diluted $TiF_4$−HCl aqueous solution,[1c,4] our self-etching process is large-scale and swift.

To demonstrate engineering applicability of the present mesoporous F−$TiO_2$ hollow microspheres for concurrent photocatalysis and membrane water treatment, we used methyl blue (MB) as a probe molecule to compare the photocatalytic activity and the membrane filtration performance with the commercially available Degussa P25 $TiO_2$ (average particle size: 25 nm). Figure S8 shows the UV−visible spectra of mesoporous F−$TiO_2$ hollow microspheres and P25. The absorption spectrum of the hollow microspheres exhibits a stronger adsorption in the UV−visible range of 325−800 nm than that of P25. Clearly, the hollow inner structure associated with accessible mesopores at the spherical surface allow the light-scattering inside their pore channels as well as their interior hollows, enhancing the light harvesting and thus increase the quantity of photogenerated electrons and hole to participate in the photocatalytic decomposition of the contaminants.[9] The removal rates of MB over the course of the photocatalytic degradation reaction are shown in Figure 3a, which indicates that with identical UV-light exposure of 6 h, the mesoporous F−$TiO_2$ hollow microspheres show higher photocatalytic activity in the degradation of MB than that of P25. The total organic carbon (TOC) removal rate also reveals that the photocatalytic decomposition rate of the mesoporous F−$TiO_2$ hollow microspheres was superior to that of P25. The enhanced photocatalytic activities of the mesoporous F−$TiO_2$ hollow microspheres can be attributed to the combined effects of several factors, namely, the surface fluorination, the existence of accessible mesopore channels, and the increased light-harvesting abilities. The treated MB aqueous solutions with suspended $TiO_2$ were filtered through the membrane cell equipped with a microfiltration membrane (MF, 0.2 $\mu$m) to recycle the

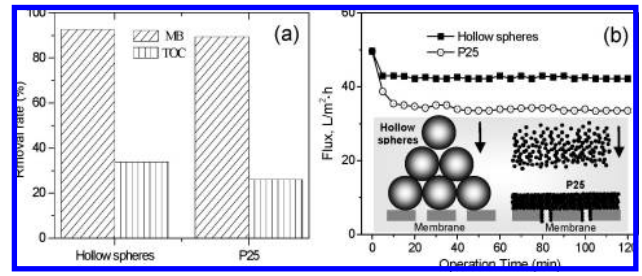


***Figure 3.*** (a) MB, TOC removal, and (b) membrane flux over mesoporous F−$TiO_2$ hollow microspheres and P25. Insert of panel b: Schematic diagram of membrane fouling caused by photocatalysts.

photocatalysts. Figure 3b shows the change in membrane flux of hollow microspheres and P25 suspension during the crossflow MF process. After 2 h of filtration, the membrane permeate flux decreased by 31.5% for P25, whereas there was only a decrease of 14.9% for the mesoporous F−$TiO_2$ hollow microspheres. The lesser membrane fouling caused by hollow microspheres is due to their mesoporous morphology and, more important, larger particle size: (1) Membrane pore blocking is totally avoided because F−$TiO_2$ hollow microspheres are unable to enter into the MF membrane pores whose size is approximately 10 times smaller than their spherical diameter. (2) Channels in the cake layer accumulated by mesoporous F−$TiO_2$ hollow microspheres on membrane surface are bigger than these in the cake layer accused by nanosized P25.[6] (Figure S9 and schematic diagram in Figure 3b)

In conclusion, hierarchically mesoporous F-$TiO_2$ hollow microspheres were prepared by precise control of $H_2SO_4$ concentration via a self-etching process. They exhibited excellent performances in concurrent membrane filtration and photocatalysis, which would be potentially useful and widely applicable in advanced photocatalytic membrane water treatment engineering. Further studies will concern their suspension characteristics and membrane antifouling property.

**Acknowledgment.** This work was supported by Prime Minister's Office of Singapore via an initiative called The Enterprise Challenge (Grant No. P00579/1273) and Public Utilities Board of Singapore. We would also like to thank FACTS for the use of FE-SEM and TEM.

**Supporting Information Available:** Experimental details and the analysis of microspheres. This material is available free of charge via the Internet at http://pubs.acs.org.

## References

(1) (a) Sun, Y.; Xia, Y. *Science* **2002**, *298*, 2176. (b) Goldberger, J.; He, R.; Zhang, Y.; Lee, S.; Yan, H.; Choi, H.-J.; Yang, P. *Nature* **2003**, *422*, 599. (c) Liu, B.; Zeng, H. C. *J. Am. Chem. Soc.* **2004**, *126*, 16744.
(2) (a) Li, H.; Bian, Z.; Zhu, J.; Zhang, D.; Li, G.; Huo, Y.; Li, H.; Lu, Y. *J. Am. Chem. Soc.* **2007**, *129*, 8406. (b) Kim, Y. J.; Chai, S. Y.; Lee, W. I. *Langmuir* **2007**, *23*, 9567. (c) Zhong, Z.; Yin, Y.; Gates, B.; Xia, Y. *Adv. Mater.* **2000**, *12*, 206.
(3) (a) Nishimura, S.; Abrams, N.; Lewis, B. A.; Halaoui, L. I.; Mallouk, T. E.; Benkstein, K. D.; van de Lagemaat, J.; Frank, A. J. *J. Am. Chem. Soc.* **2003**, *125*, 6306. (b) Koo, H. J.; Kim, Y. J.; Lee, Y. H.; Lee, W. I.; Kim, K.; Park, N. G. *Adv. Mater.* **2008**, *20*, 195.
(4) (a) Li, J.; Zeng, H. C. *J. Am. Chem. Soc.* **2007**, *129*, 15839. (b) Yang, H. G.; Zeng, H. C. *J. Phys. Chem. B* **2004**, *108*, 3492.
(5) (a) Liu, Z.; Wu, P.; Sun, D. D.; Leckie, J. O. *Chem.—Eur. J.* **2007**, *13*, 1851. (b) Yu, J.; Liu, S.; Yu, H. *J. Catal.* **2007**, *249*, 59.
(6) (a) Tang, C. Y.; Kwon, Y. N.; Leckie, J. O. *Environ. Sci. Technol.* **2007**, *41*, 942. (b) Huang, H.; Young, T. A.; Jacangelo, J. G. *Environ. Sci. Technol.* **2008**, *42*, 714.
(7) Sun, D. D.; Lee P. F.; Leckie, J. O. U.S. Patent Provisional 60/870,939 t, 2006.
(8) Park, H.; Choi, W. *J. Phys. Chem. B* **2004**, *108*, 4086.
(9) Yu, J. C.; Yu, J.; Ho, W.; Jiang, Z.; Zhang, L. *Chem. Mater.* **2002**, *14*, 3808.

JA803582M